

Geophysical Research Letters®

RESEARCH LETTER

10.1029/2021GL096520

Key Points:

- Oxalate-sulfate mass ratios show similarity across multiple environments (95% confidence interval: 0.0154–0.0296; $R = 0.76$; $N = 2,948$)
- Oxalate-sulfate mass ratio is biased toward higher values in presence of coarse aerosol particles and/or biomass burning
- Ground-based, size-resolved measurements reveal that the ratio can be robust within the mixed layer for the submicrometer mode

Supporting Information:

Supporting Information may be found in the online version of this article.

Correspondence to:












A. Sorooshian,
armin@email.arizona.edu

Citation:

Hilario, M. R. A., Crosbie, E., Bañaga, P. A., Betito, G., Braun, R. A., Cambaliza, M. O., et al. (2021). Particulate oxalate-to-sulfate ratio as an aqueous processing marker: Similarity across field campaigns and limitations. *Geophysical Research Letters*, 48, e2021GL096520. <https://doi.org/10.1029/2021GL096520>

Received 7 OCT 2021
Accepted 20 NOV 2021

Particulate Oxalate-To-Sulfate Ratio as an Aqueous Processing Marker: Similarity Across Field Campaigns and Limitations

Miguel Ricardo A. Hilario¹ , Ewan Crosbie^{2,3} , Paola Angela Bañaga^{4,5}, Grace Betito^{4,5}, Rachel A. Braun^{6,7} , Maria Obiminda Cambaliza^{4,5}, Andrea F. Corral⁶ , Melliza Templonuevo Cruz^{4,8} , Jack E. Dibb⁹ , Genevieve Rose Lorenzo¹, Alexander B. MacDonald⁶ , Claire E. Robinson^{2,3}, Michael A. Shook² , James Bernard Simpas^{4,5}, Connor Stahl⁶, Edward Winstead^{2,3} , Luke D. Ziemba² , and Armin Sorooshian^{1,6} 

¹Department of Hydrology and Atmospheric Sciences, University of Arizona, Tucson, AZ, USA, ²NASA Langley Research Center, Hampton, VA, USA, ³Science Systems and Applications, Inc., Hampton, VA, USA, ⁴Manila Observatory, Quezon City, Philippines, ⁵Department of Physics, School of Science and Engineering, Ateneo de Manila University, Quezon City, Philippines, ⁶Department of Chemical and Environmental Engineering, University of Arizona, Tucson, AZ, USA, ⁷Now at: Healthy Urban Environments Initiative, Global Institute of Sustainability and Innovation, Arizona State University, Tempe, AZ, USA, ⁸Institute of Environmental Science and Meteorology, University of the Philippines, Diliman, Quezon City, Philippines, ⁹Earth Systems Research Center, Institute for the Study of Earth, Oceans, and Space, University of New Hampshire, Durham, NH, USA

Abstract Leveraging aerosol data from multiple airborne and surface-based field campaigns encompassing diverse environmental conditions, we calculate statistics of the oxalate-sulfate mass ratio (median: 0.0217; 95% confidence interval: 0.0154–0.0296; $R = 0.76$; $N = 2,948$). Ground-based measurements of the oxalate-sulfate ratio fall within our 95% confidence interval, suggesting the range is robust within the mixed layer for the submicrometer particle size range. We demonstrate that dust and biomass burning emissions can separately bias this ratio toward higher values by at least one order of magnitude. In the absence of these confounding factors, the 95% confidence interval of the ratio may be used to estimate the relative extent of aqueous processing by comparing inferred oxalate concentrations between air masses, with the assumption that sulfate primarily originates from aqueous processing.

Plain Language Summary The extent of atmospheric chemical processing remains an uncertain aspect of air mass characterization. Addressing this uncertainty is important because chemical reactions in the atmosphere in the presence of water (aqueous processing) produce a large fraction of global aerosol mass. The oxalate-to-sulfate ratio has been proposed as an indicator of aqueous processing, where higher values point to increased processing of an air mass. In this study, we quantify a range in the oxalate-to-sulfate mass ratio (0.0154–0.0296) using data from multiple field campaigns encompassing a diverse set of environments. This range is robust near the surface for particles below 1 micrometer in diameter. Larger particles, especially dust, and biomass burning particles significantly affect the oxalate-to-sulfate ratio and thus may confound the interpretation of a high oxalate-to-sulfate ratio as a signal of aqueous processing. In the absence of dust and biomass burning particles, the oxalate-to-sulfate ratio range may be used to compare the relative extent of aqueous processing between different air masses.

1. Introduction

Organic aerosol (OA) account for a major fraction of atmospheric aerosol particles (Hallquist et al., 2009; Kanakidou et al., 2005; Zhang et al., 2007) comprising between 20% and 50% of fine aerosol mass in the continental mid-latitudes (Putaud et al., 2004; Saxena & Hildemann, 1996), 30%–80% in the free troposphere (Murphy et al., 2006), and over 80% in tropical forests (Andreae & Crutzen, 1997; Roberts et al., 2001). Secondary organic aerosol (SOA) are derived from gas-to-particle conversion processes, including aqueous processing (Blando & Turpin, 2000; Ervens et al., 2011; Warneck, 2003), wherein oxidized volatile organic compounds (VOCs) partition into cloud droplets or wet aerosol particles and undergo chemical reactions to form low-volatility products that remain in the condensed phase (Ervens, 2015; Ervens et al., 2011; McNeill, 2015). The formation of SOA through aqueous processing has been estimated to serve as a global SOA source comparable to the gas-phase pathway, with 90% of aqueous-phase SOA formed in-cloud (Fu et al., 2008). Using the scheme from Fu

et al. (2008), Heald et al. (2011) found contributions of SOA to total OA ranging between 20% and 80% across environments. Oxygenated organic species comprise 60%–95% of total organic aerosol mass across urban and remote sites (Zhang et al., 2007), while SOA from VOCs explains up to 70% of global organic carbon mass (Hallquist et al., 2009). More recent work reports reduced discrepancy between models and observations for SOA concentrations (Hodzic et al., 2016; Pai et al., 2020; Zhu & Penner, 2019). However, despite improvements in modeling organic aerosol (Heald et al., 2005, 2011), atmospheric chemistry models still underestimate SOA (Schroder et al., 2018) due partly to an incomplete understanding and representation of aqueous processes, resulting in poor model parameterization (Hallquist et al., 2009; McNeill, 2015). The inclusion of SOA formation by aqueous phase processes has been shown to decrease model bias (−64%–15%) and increase model correlations with observations ($R = 0.5$ – 0.6) (Carlton et al., 2008); thus, improving SOA estimates is a key area of development for models to more accurately evaluate the impacts of atmospheric aerosol particles and reduce uncertainties regarding the net effect of aerosol particles on health and climate (Intergovernmental Panel on Climate Change, 2014).

Oxalic acid is the most abundant organic acid in tropospheric aerosol particles across different regions (Cruz et al., 2019; Yang et al., 2014; Ziemba et al., 2011). The ion oxalate (OXL) is a well-established tracer of aqueous processing, contributing 1%–10% of total particulate mass (Ervens, 2015; Myriokefalitakis et al., 2011) and 3%–4% of total organic mass over marine/continental areas (Sorooshian et al., 2010). OXL is often used in combination with other secondary tracers such as sulfate (SO_4^{2-}) to assess the extent of aqueous processing in a region (Crahan et al., 2004; Hilario, Cruz, Bañaga, et al., 2020; Sorooshian, Varutbangkul, et al., 2006; Wang et al., 2012; Yu et al., 2005). Direct sources are thought to be minor relative to production via aqueous processing (Ervens, 2015; Huang & Yu, 2007; Myriokefalitakis et al., 2011) and photochemistry (Zhang et al., 2020). Sources of gaseous OXL precursors include biomass burning (BB) (Narukawa et al., 1999; Yang et al., 2014) and biogenic emissions (Boone et al., 2015). Early model simulations overestimated OXL by an order of magnitude (Crahan et al., 2004) while global simulations by Myriokefalitakis et al. (2011) showed better agreement over marine/rural environments between observed and modeled OXL (modeled:observed slope = 1.16 ± 0.14 ; $R = 0.60$) but could not capture OXL over urban regions (weak correlation; $r \approx 0$).

The OXL: SO_4^{2-} ratio has been suggested in past work to be an indicator of aqueous processing (Ervens et al., 2014; Wonaschuetz et al., 2012; Yu et al., 2005). The usage of the ratio as an aqueous processing marker implies that OXL and SO_4^{2-} are entirely sourced from aqueous-phase oxidation, whether it be in cloud droplets or wet aerosol particles, and does not account for gas-phase oxidation in cloud-free air (Ervens, 2015; D. D.; Huang et al., 2020; Zhan et al., 2021) or direct emissions of OXL (Chebbi & Carlier, 1996). This is a good assumption for OXL as there is thought to be no gas-phase reaction that would produce OXL (i.e., an aqueous medium is required for OXL production) (Warneck, 2003); however, OXL is influenced by gas-particle partitioning equilibrium and can exist in the gas-phase as oxalic acid (Nah et al., 2018; Tao & Murphy, 2019). For SO_4^{2-} , gas-phase oxidation is an important source of uncertainty as it can dominate over aqueous processing at times (D. D. Huang et al., 2020). Though we also note that oxidation in the gas-phase is much slower than in the aqueous-phase (Cautenet & Lefeuvre, 1994) and aqueous-phase oxidation explains 60%–90% of SO_4^{2-} in global models (Barth et al., 2000; Faloon, 2009; Fu et al., 2008).

The OXL: SO_4^{2-} ratio can serve as an aqueous processing marker because aqueous media (including clouds and wet aerosol particles) facilitate the production of both OXL and SO_4^{2-} at rates dependent on liquid water content for SO_4^{2-} formation and droplet surface area for OXL (Ervens et al., 2014; McVay & Ervens, 2017). These two cloud parameters correlate within growing clouds (Kim et al., 2003), which connects in-cloud OXL and SO_4^{2-} production. The OXL: SO_4^{2-} ratio has been observed to correlate well with cloud fraction and fall within 0.01–0.03 between 0 and 4 km above ground level (AGL) when cloud fractions are high (Wonaschuetz et al., 2012). Therefore, identifying a range in the OXL: SO_4^{2-} ratio across different environments can be useful for comparing relative extents of aqueous processing with higher ratios suggesting more processed air. This comes with the assumptions outlined above that SO_4^{2-} is mainly sourced from aqueous processing, which may not hold for certain environments. However, this ratio is expected to be particularly applicable near clouds. It is important to note that this ratio likely exhibits a seasonal cycle as observed in Tao and Murphy (2019). Work by Yao et al. (2004) also demonstrated seasonal shifts in the relative contributions of primary and secondary OXL.

Laboratory experiments are often relied on for mechanistic details of aerosol particles (e.g., Hennigan et al., 2010; Pang et al., 2019) but sometimes disagree with aircraft measurements (May et al., 2014). Thus, aircraft campaigns

provide a valuable opportunity to study aerosol particles influenced by cloud processes in their most natural environment (Sorooshian et al., 2020). This study leverages composition data from multiple field campaigns, predominantly based on airborne measurements, to investigate the following questions: (a) Is there a generally consistent range of OXL:SO₄²⁻ across different regions? (b) does this ratio depend on particle size? and (c) what conditions can significantly affect OXL:SO₄²⁻ values?

2. Methods

This work relies mostly on airborne field datasets, focusing mainly on particle-into-liquid sampler (PILS) data. The PILS converts sampled aerosol particles into droplets sufficiently large to be collected via inertial impaction, with the resultant liquid transported to vials on a rotating carousel for post-collection chemical analysis via ion chromatography (IC) (Sorooshian, Brechtel, et al., 2006; Weber et al., 2001).

Table 1 summarizes relevant details across campaigns, namely: the International Consortium for Atmospheric Research on Transport and Transformation (ICARTT), the Marine Stratus/Stratocumulus Experiment (MASE-I), the Gulf of Mexico Atmospheric Composition and Climate Study (GoMACCS), the Marine Stratus/Stratocumulus Experiment II (MASE-II), the Nucleation in California Experiment (NiCE), the Atmospheric Tomography Mission (AToM), the Cloud, Aerosol, and Monsoon Processes-Philippines Experiment (CAMP²Ex), the ground-based CAMP²Ex weatHER and CompoSition Monitoring (CHECSM) study, and the Aerosol Cloud meTeorology Interactions oVer the western ATlantic Experiment (ACTIVATE). Note that species from AToM were collected by Soluble Acidic Gases and Aerosol (SAGA) filters (Dibb et al., 2002, 2003). We use ground-based data from Metro Manila, Philippines during CHECSM collected by a micro-orifice uniform deposit impactor (MOUDI) and analyzed via IC to assess how the OXL:SO₄²⁻ ratio may vary within the mixed layer and across particle sizes. We examined a total of 53 MOUDI sets that were collected on a weekly basis with a sample duration of ~48 hr per set. Six of those sets were impacted by BB based on the criteria presented by Gonzalez et al. (2021) for the same data set.

As we analyze a CAMP²Ex case study in Section 3.2, we summarize the campaign here with more details provided in Hilario et al. (2021). CAMP²Ex took place over the Western Pacific and aimed to study the influence of radiation, convection, and meteorology on aerosol and gas species. With 19 research flights from August–October 2019, CAMP²Ex provided a rich composition, radiation, and convection dataset spanning 0–9 km AGL. In this study, we analyze submicrometer non-refractory aerosol from the aerosol mass spectrometer (AMS; Aerodyne) (Canagaratna et al., 2007; DeCarlo et al., 2006) and size distributions collected by a laser aerosol spectrometer (LAS; TSI Model 3340) for particle diameters 50–3162 nm. A comparison of SO₄²⁻ from the PILS and AMS during CAMP²Ex shows good agreement (AMS:PILS slope = 0.81; R = 0.88), suggesting that SO₄²⁻ was predominantly in the submicrometer size range given the size ranges of the AMS (PM₁) and PILS (PM_{~4}). Based on sea salt SO₄²⁻ calculations, less than 5% of SO₄²⁻ during CAMP²Ex originated from sea salt.

During AToM, CAMP²Ex, and ACTIVATE, the aerosol sampling inlet likely limited the upper size to approximately 4 μm (McNaughton et al., 2007) although there may have been additional impaction losses in the sampling lines internal to the aircraft that further smoothed the particle transmission curve near this upper bound. This higher cutoff size allowed for sampling of sea salt and dust.

To meaningfully compare OXL:SO₄²⁻ ratios between campaigns, we separated out samples impacted by strong point sources (e.g., ship plumes, cattle feedlots, smoke) as identified using flight scientist notes and clear enhancements in particle concentration data. When calculating species ratios, we excluded instances when the denominator value was below its fifth percentile to reduce the uncertainty caused by low denominator values. Ratios of species in this study refer to mass ratios unless otherwise indicated (e.g., molar ratios). To quantify an all-campaign statistic and uncertainty, median and 95% confidence intervals of the OXL:SO₄²⁻ ratio were derived via bootstrapping of all campaigns using different combinations of sample size and number of iterations, excluding samples with confounding influence (further details are provided in Table S1 in Supporting Information S1).

Table 1
Details of Aircraft Campaigns Analyzed

	Location	Location characteristics	Years analyzed	Maximum altitude (km AGL)	Size range	Slope (R; N) Non-BB	Slope (R; N) BB	Campaign reference
ICARTT	Ohio River Valley, USA	Continental	August 2004	3	PM ₁	0.0259 ± 0.0311 (0.85; 142)	–	Fehsenfeld et al. (2006) Sorooshian, Varutbangkul et al. (2006)
MASE-I	Northeast Pacific Ocean	Coastal	July 2005	3.5	PM ₁	0.0233 ± 0.0092 (0.51; 214)	–	Lu et al. (2007)
GoMACCS	Texas, USA	Continental	August – September 2006	5	PM ₁	0.0167 ± 0.0253 (0.63; 867)	–	Sorooshian, Lu, et al. (2007) Parrish et al. (2009)
MASE-II	Northeast Pacific Ocean	Coastal	July 2007	2.5	PM ₁	0.014 ± 0.0085 (0.31; 438)	–	Sorooshian, Ng, et al. (2007) Lu et al. (2009)
NiCE	Northeast Pacific Ocean	Coastal	July–August 2013	3	PM ₁	0.0189 ± 0.0039 (0.42; 67)	0.0244 ± 0.0037 (0.25; 27)	Sorooshian et al. (2009) Sorooshian et al. (2015)
AToM	Pacific Ocean (50°S to 50°N; 155°E to 235°E)	Marine	2016–2018	12	PM _{–4}	0.0265 ± 0.0052 (0.72; 124)	–	Wofsy et al. (2018)
CHECSM	Metro Manila, Philippines	Coastal/Urban	2018–2019	Surface (85 m AGL)	PM ₁₈	0.0264 ± 0.0255 (0.73; 47)	0.1426 ± 0.0778 (0.82; 6)	Stahl et al. (2020a)
CAMP ² Ex	West Pacific Ocean	Marine/Coastal	August–October 2019	9	PM _{–4}	High-OXL: 0.3497 ± 0.063 (0.27; 109) High-SO ₄ ²⁻ : 0.0035 ± 0.0106 (0.43; 447)	0.048 ± 0.0462 (0.84; 94)	Hilario et al. (2021)
ACTIVATE	Northwest Atlantic Ocean	Coastal	August–September 2020	5	PM _{–4}	0.0167 ± 0.0132 (0.42; 273)	–	Sorooshian et al. (2019)

Note. Statistics of oxalate (OXL) and sulfate (SO₄²⁻) from Figure 1 are listed (R = Pearson correlation, N = number of samples). Median absolute deviation (MAD) is provided as a measure of slope uncertainty (e.g., slope ± MAD; r, N). Statistics are presented separately for biomass burning (BB) and non-biomass burning (non-BB) samples.

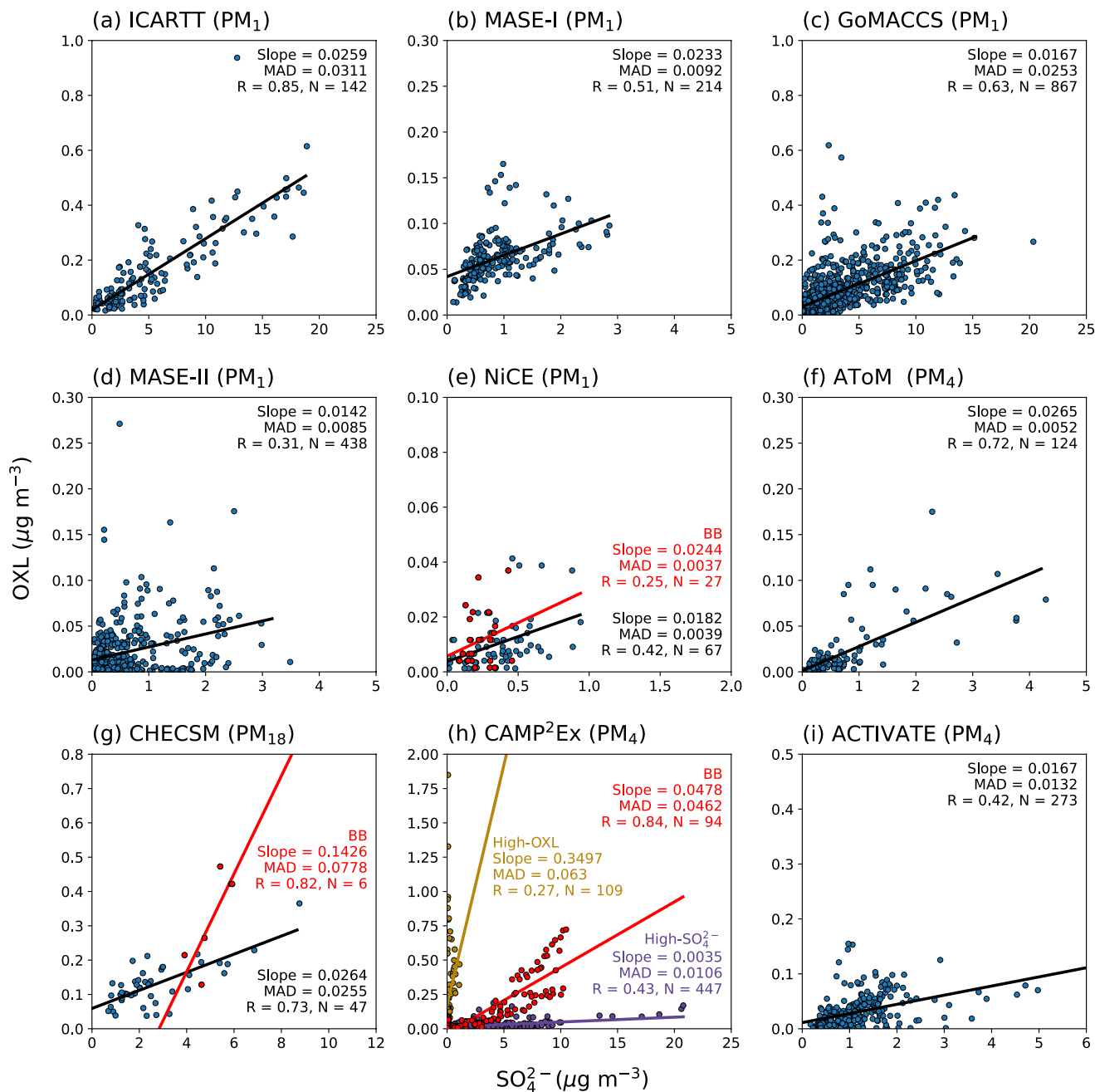


Figure 1. Linear regressions of oxalate (OXL) and SO_4^{2-} mass concentrations across different field campaigns sorted chronologically. All campaigns are aircraft-based except for the Cloud, Aerosol, and Monsoon Processes-Philippines Experiment (CAMP²Ex) weaTHER and CompoSition Monitoring (CHECSM; g), which was ground-based. Statistics for BB-impacted samples are presented separately in red. CAMP²Ex high-OXL and high- SO_4^{2-} populations are colored in yellow and purple, respectively, in (h). Axes limits are not standardized across panels. In addition to Pearson's R, the median absolute deviation (MAD) was used as a measure of slope goodness-of-fit.

3. Results

3.1. Statistics of the OXL: SO_4^{2-} Ratio

Across multiple environments (Figure 1), we observe similarities in the range of the OXL: SO_4^{2-} ratio (i.e., slope) across campaigns except for CAMP²Ex (discussed in Section 3.2). A combined plot of all campaigns suggests a common range of OXL: SO_4^{2-} across different environments (Figure S1 in Supporting Information S1). Visually,

the range in OXL:SO₄²⁻ (Figure S1 in Supporting Information S1) decreases with increasing concentrations, perhaps from a clearer signal of aqueous processing at higher concentrations.

Bootstrapping across all campaigns reveals a stable median OXL:SO₄²⁻ of 0.0217 ($R = 0.76$; $N = 2948$) (details in Table S1 in Supporting Information S1) with 95% confidence interval bounds (0.0154–0.0296) indicating a relative uncertainty range of $\sim\pm 30\%$ around the median. The bootstrapped statistics are supported by averaging the OXL:SO₄²⁻ slopes between campaigns in Figure 1 (mean: 0.0184, standard deviation: 0.007, median absolute deviation (MAD): 0.004), which, similar to our bootstrapping method, weights all campaigns equally and removes the statistical bias toward larger datasets. The bootstrapped 95% confidence interval of our observed OXL:SO₄²⁻ (0.0154–0.0296) is in excellent agreement with the ratio of yields between aqueous SOA (0.008–0.033; Ervens et al., 2011) and SO₄²⁻ (approximately unity), corroborating the hypothesis of a general range in OXL:SO₄²⁻. Numerous studies spanning a diverse set of environments have reported OXL:SO₄²⁻ values (Table S2 in Supporting Information S1) with several falling within our bootstrapped range.

Cumulative probability functions (CDFs) were plotted to more easily compare OXL:SO₄²⁻ between campaigns (Figure S2 in Supporting Information S1). As point-by-point ratios are sensitive to background levels of OXL and SO₄²⁻, we plotted CDFs of their enhancement ratio ($\Delta\text{OXL}/\Delta\text{SO}_4$) where values were subtracted by their tenth percentile to approximate background levels per campaign. The resulting CDFs showed similar curves between multiple campaigns and revealed that approximately 20% of point-by-point OXL:SO₄²⁻ values fall within our bootstrapped 95% confidence interval (0.0154–0.0296) while $\sim 50\%$ of OXL:SO₄²⁻ values fall within 0.010–0.050. In comparison with the linear regression slope, point-to-point ratios are more susceptible to differences in background, resulting in differences in agreement with our 95% confidence interval (e.g., CHECSM). This is a consequence of the point-by-point calculation: although the data set as a whole may have a mean slope within our confidence interval, there may still be variability in the OXL:SO₄²⁻ ratios of individual points. Thus, as the tenth percentile merely accounts for campaign backgrounds, the linear regression slopes (Figure 1) may better handle different environments by implicitly accounting for individual background levels via non-zero intercepts.

Surface OXL:SO₄²⁻ values from CHECSM agree with the bootstrapped 95% confidence interval for non-BB samples for PM₁₈ (0.0264; Figure 1g) and PM₁ (0.0196) modes ($R = 0.73$ for both). Size-resolved data show that this agreement is greatest between 0.32–1 μm (Figure S3a in Supporting Information S1), where OXL and SO₄²⁻ masses mostly reside (Cruz et al., 2019). An increase in supermicrometer OXL:SO₄²⁻ (Figure S3a in Supporting Information S1) suggests the enhancement of OXL via gas-particle partitioning of OXL and/or its precursors onto coarse particles as documented for the CHECSM region (Stahl et al., 2020b, 2021). These results suggest the ratio may be applicable to the mixed layer for submicrometer particles.

AToM provides insight into the OXL:SO₄²⁻ ratio over remote marine environments in both hemispheres. The Pacific and Atlantic Oceans (<3 km AGL) have a combined OXL:SO₄²⁻ ratio of 0.0207 ($R = 0.51$) (Figure 1f). Separately, the Pacific and Atlantic have ratios of 0.0180 ($R = 0.36$) and 0.0251 ($R = 0.72$), respectively, remarkably similar to other environments (Figure 1). Across altitudes (Figure S4 in Supporting Information S1), OXL:SO₄²⁻ values for the Pacific between 0 and 7.5 km AGL are within our 95% confidence interval (Figure S4a in Supporting Information S1) but only near-surface Atlantic samples fall within our confidence interval (Figure S4c in Supporting Information S1), possibly due to OXL and/or its precursors undergoing gas-particle partitioning onto Saharan dust.

Variability in OXL:SO₄²⁻ across campaigns was most evident in MASE-II (Figure 1d) and CAMP²Ex (Figure 1h), which had instances of very low OXL:SO₄²⁻, attributable to (a) fresher plumes that have not had time to form OXL (Wonaschuetz et al., 2012), (b) the degradation of OXL into CO₂ (Zhou et al., 2020), (c) the formation of OXL-metal complexes (Sorooshian et al., 2013; Tao & Murphy, 2019), and (d) the presence of high SO₄²⁻ backgrounds. Correlation coefficients below 0.50 (Figure 1) signify the presence of confounding sources, an expected result given the diversity of environments analyzed. Seasonal factors may also influence the ratio (Tao & Murphy, 2019). Variability between campaigns (Figure 1) may be suggestive of SO₄²⁻ from cloud-free photochemistry and gas-phase oxidation (Ervens, 2015), which are important sources of uncertainty when using the OXL:SO₄²⁻ ratio to assess aqueous processing, as our proposed range implies that SO₄²⁻ is mainly from aqueous processing.

The main utility of this ratio is to gauge relative rather than absolute extents of aqueous processing between air masses via a comparison of inferred OXL. Considering the differences between OXL and SO₄²⁻ in terms of their

precursors, formation mechanisms, and sinks, the consistency of the OXL:SO₄²⁻ ratio across multiple environments implies a convergence toward a fairly narrow range, which is assisted in part by the large sample sizes used in this study.

3.2. Source of the CAMP²Ex High-OXL Population

Oxalate and SO₄²⁻ from CAMP²Ex show three populations: high-OXL, high-SO₄²⁻, and BB-impacted, each characterized by a distinct OXL:SO₄²⁻ slope (Figure 1h). BB-impacted samples are defined as data collected during RFs 9 and 10 (15 and 16 September 2019, respectively), which targeted smoke emissions. The high-OXL population was defined with OXL:SO₄²⁻ > 0.3 and the high-SO₄²⁻ population with OXL:SO₄²⁻ < 0.06; varying the high-OXL ratio lower threshold within 0.10–0.30 and high-SO₄²⁻ upper threshold within 0.06–0.10 does not impact results of the analyses presented below. Ensuing discussion about these three populations points to important influences on the OXL:SO₄²⁻ ratio.

The high-OXL population during CAMP²Ex (Figure 1h) was not observed in the other field campaigns. These high-OXL samples were mostly sampled within the free troposphere (>5 km) (Figure S5b in Supporting Information S1), altitudes of which were rarely sampled in other field campaigns with AToM being the exception. A few reasons can explain the high-altitude, high-OXL samples during CAMP²Ex: (a) OXL's lengthier chemical formation pathways compared to SO₄²⁻ (Ervens, 2015; Sorooshian, Lu, et al., 2007), (b) inefficient scavenging of gaseous precursors as air masses are transported upward (Heald et al., 2005), and (c) gas-phase OXL and/or its precursors partitioning onto dust particles (Stahl et al., 2020b, 2021; Sullivan & Prather, 2007). As the PILS sampled PM₄ during CAMP²Ex, we hypothesize that the enhanced OXL is due to gas-particle partitioning of OXL and/or its precursors onto coarse mode particles such as dust or sea salt (Mochida et al., 2003; Rinaldi et al., 2011; Sullivan & Prather, 2007; Turekian et al., 2003), evidenced by a prominent coarse mode peak ($D_p \sim 2.5 \mu\text{m}$) in the size distributions of high-OXL samples (Figure S5 in Supporting Information S1). Among the two sources, dust is more likely based on the higher affinity of OXL and/or its precursors to partition onto dust particles compared to sea salt particles (Stahl et al., 2020b). Furthermore, efficient wet scavenging of sea salt reduces its free troposphere concentrations as compared to those of the marine boundary layer (Murphy et al., 2019; Schlosser et al., 2020).

Though both AToM and CAMP²Ex sampled a wide range of altitudes, no high-OXL population was observed during AToM. This is because CAMP²Ex operated near major dust sources such as the Maritime Continent (Hilario, Cruz, Cambaliza, et al., 2020) and continental Asia (Matsumoto et al., 2003) while data from AToM represent more remote marine environments (Table 1). Though the OXL:SO₄²⁻ ratio from AToM is indeed slightly enhanced aloft over the Atlantic (Figure S4c in Supporting Information S1), this is still a full order of magnitude lower than that of the high-OXL population from CAMP²Ex (Figure 1h).

To more deeply characterize the high-OXL population, we compared several key variables between the CAMP²Ex high-OXL and high-SO₄²⁻ populations (Table S3 in Supporting Information S1), all of which showed statistically significant differences based on the Mann-Whitney U-test (99% confidence level; $p < 0.01$). The following characteristics hint to gas-particle partitioning of OXL and/or its precursors onto dust aloft as has been documented in other studies (e.g., Stahl et al., 2020b; Sullivan & Prather, 2007): (a) dust species such as Ca²⁺ (Kchih et al., 2015) had approximately double the mass concentration in high-OXL air as compared to high-SO₄²⁻ air (Table S3 in Supporting Information S1), (b) high-OXL air was mostly sampled in the free troposphere (Figure S5 in Supporting Information S1), (c) ionic crustal ratios in the free troposphere (>5 km) were more similar to dust values than those for sea salt based on literature (Park et al., 2004; Švédová et al., 2019; Wang et al., 2018) (Figure 2), and (d) a prominent coarse mode peak is observed for high-OXL samples (Figure S6 in Supporting Information S1). Among the other two campaigns sampling PM₄, elevated OXL:SO₄²⁻ values at higher altitudes were also observed during AToM (Figure S4 in Supporting Information S1); during ACTIVATE, dust was not prevalent at the altitudes sampled (<5 km).

We next compared m/z 44_{AMS} and OXL (from PILS) to assess the possibility of gas-particle partitioning of OXL and/or its precursors onto coarse mode particles such as dust. m/z 44_{AMS} indicates the mass concentration of oxygenated/aged organic aerosol with the functional group CO₂⁺ (Zhang et al., 2005), of which OXL is a sub-component. As the AMS sampled PM₁ and the PILS sampled PM₄ in CAMP²Ex, their comparison lends insight into how coarse mode particles (i.e., 1–4 μm) may affect PILS observations. Furthermore, because OXL is one

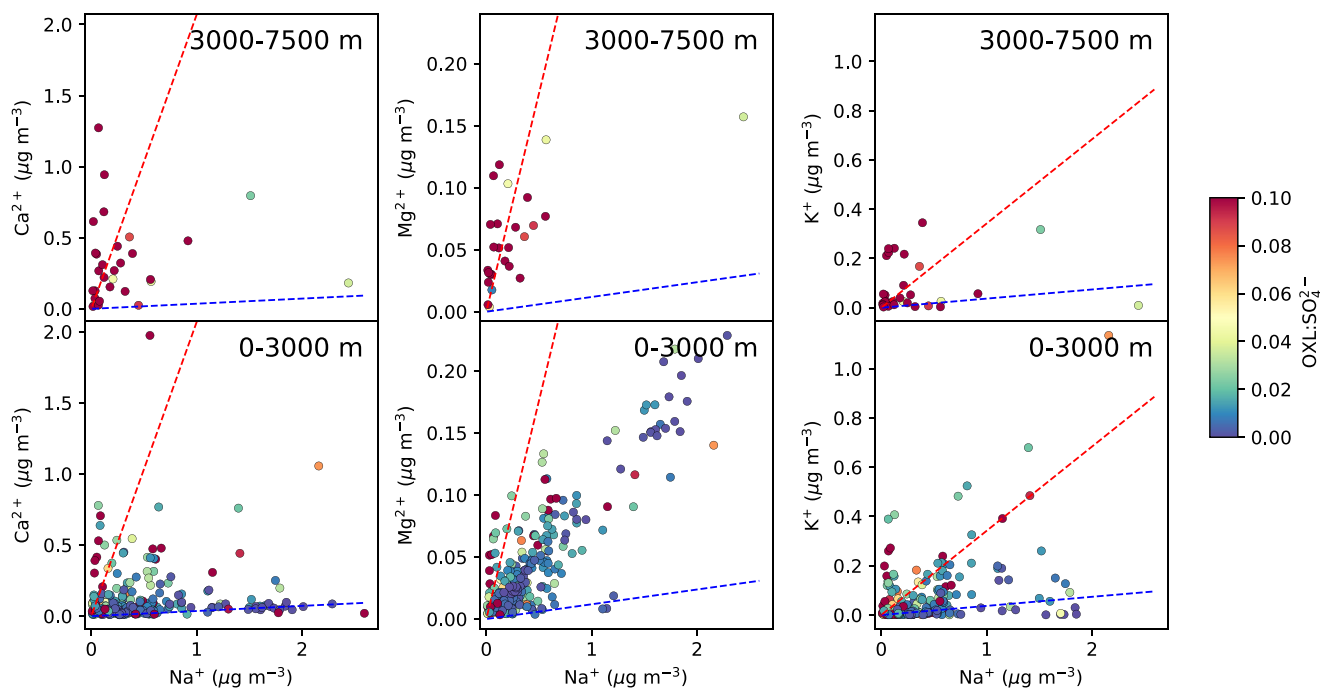


Figure 2. Altitude-resolved linear regressions of dust species collected by the particle-into-liquid sampler during the Cloud, Aerosol, and Monsoon Processes-Philippines Experiment (BB samples excluded) colored by $\text{OXL}:\text{SO}_4^{2-}$. Red and blue dashed lines denote literature-based ratios for dust (Park et al., 2004; Švédová et al., 2019; Wang et al., 2018) and sea salt (Chesselet et al., 1972), respectively.

component of m/z 44_{AMS}, comparing PILS OXL (PM_4) to m/z 44_{AMS} (PM_1) can serve as an indicator of coarse mode OXL if $\text{OXL}:m/z$ 44_{AMS} ≈ 1 as a highly conservative threshold. The high-OXL population has an $\text{OXL}:m/z$ 44_{AMS} molar ratio of 2.84 ± 3.95 (Table S3 in Supporting Information S1), which provides strong evidence for coarse mode OXL (1–4 μm). This is supported by a high $\text{OXL}:\text{Org}_{\text{AMS}}$ ratio in the high-OXL population (0.84 ± 0.98) compared to the high- SO_4^{2-} population (0.01 ± 0.01). Interestingly, $\text{Org}_{\text{AMS}}:\text{SO}_4^{2-}$ is similar between the high-OXL (1.08 ± 1.34) and high- SO_4^{2-} populations (1.27 ± 1.02). Since the AMS samples PM_1 , these findings offer more evidence that differences between populations lie in the coarse mode.

3.3. Impact of Biomass Burning on $\text{OXL}:\text{SO}_4^{2-}$

Although strong OXL and SO_4^{2-} correlations may be interpreted as a signal of aqueous processing (Sorooshian, Varutbangkul, et al., 2006; Yao et al., 2003; Yu et al., 2005), the presence of BB emissions must also be considered as a source of both SO_4^{2-} and OXL (Narukawa et al., 1999; Yang et al., 2014). When present, BB emissions led to enhanced $\text{OXL}:\text{SO}_4^{2-}$ ratios and correlations (Figure 1). Size-resolved $\text{OXL}:\text{SO}_4^{2-}$ show similar enhancements during BB periods (Figure S3b). In the presence of BB emissions, the $\text{OXL}:\text{SO}_4^{2-}$ ratio is known to increase from 0.05 (non-BB) to 0.18 (BB) in Sydney (Swan & Ivey, 2021) and from 0.03 to 0.069 (non-BB) to 0.072–0.15 (BB) in Hong Kong (Zhou et al., 2015). Differences in BB-related $\text{OXL}:\text{SO}_4^{2-}$ between environments may be attributed to factors including biomass type (Christian et al., 2003), wet scavenging during transport (Marelle et al., 2015), combustion phase (Kondo et al., 2011; Pósfai et al., 2003), and sampled size range (i.e., PM_4 for CAMP²Ex, PM_1 for NiCE, PM_{18} for CHECSM). During CAMP²Ex, BB-impacted data suggested two subpopulations that differ slightly in their $\text{OXL}:\text{SO}_4^{2-}$ slopes (Figure 1h). Both populations were sampled during a large biomass burning event (September 15, 2019; RF9) but differ in terms of location (~330 km apart), composition, and number concentration (not shown), pointing to clear differences within the CAMP²Ex BB-impacted population left for future work. Regardless of BB differences between campaigns, such a pronounced impact on the $\text{OXL}:\text{SO}_4^{2-}$ ratio in those respective datasets demonstrates the importance of accounting for BB when exploiting the $\text{OXL}:\text{SO}_4^{2-}$ ratio for analysis and modeling purposes relevant to secondary aerosol formation processes.

4. Conclusions

Using composition data from multiple campaigns spanning a variety of environments, we calculated statistics of the OXL:SO₄²⁻ mass ratio (median: 0.0217; $R = 0.76$; $N = 2948$), with 95% confidence interval bounds indicating a relative uncertainty range of $\sim\pm 30\%$ around the median (0.0154–0.0296). Ground-based size-resolved measurements show overall agreement with the proposed range, specifically within the submicrometer mode, suggesting our results are robust within the mixed layer for PM₁. Results from remote marine measurements from AToM over the Pacific and near-surface Atlantic Oceans also corroborate the bootstrapped OXL:SO₄²⁻ range. As analyzed environments span continental and coastal North America; west, east, and central Pacific Ocean; and west and central Atlantic Ocean, the confidence interval of the ratio is proposed to be robust to a wide range of factors that can impact the formation and removal of both OXL and SO₄²⁻. Furthermore, remarkable similarity between our 95% confidence interval (0.0154–0.0296) and the ratio of yields between SO₄²⁻ and aqueous SOA (~ 0.008 – 0.033) (Ervens et al., 2011) supports the hypothesis of a generalizable range of OXL:SO₄²⁻.

One exception to the hypothesized OXL:SO₄²⁻ range was the occurrence of gas-phase OXL and/or its precursors partitioning onto dust aloft during CAMP²Ex. Additionally, BB emissions as a source of both OXL and SO₄²⁻ may produce a strong correlation and greatly elevate their ratio. Thus, we caution against interpreting a strong OXL and SO₄²⁻ correlation as a standalone signature of aqueous processing when coarse particle types (e.g., dust) and/or BB emissions are present.

Given its relative uncertainty range ($\sim\pm 30\%$ around the median) when taken across multiple environments, the 95% confidence interval of the OXL:SO₄²⁻ ratio could be used to assess the relative extent of aqueous processing by comparing inferred OXL concentrations between air masses, with the implicit assumption that sampled SO₄²⁻ mainly originates from aqueous processing, which is expected to be particularly true but not limited to near clouds. We emphasize that the OXL:SO₄²⁻ ratio applies specifically to aqueous-processed aerosol (including via clouds or wet aerosol particles) and that an estimation of total SOA from this ratio requires additional information about the ratio of OXL and SOA. Furthermore, gas-phase oxidation is an important source of uncertainty in the ratio as it can be the dominant SO₄²⁻ pathway at times and may partly explain OXL:SO₄²⁻ variability between campaigns.

Examining the OXL:SO₄²⁻ ratio in other parts of the world and seasons would be beneficial to further gauge its variability as well as to identify other potentially confounding factors. Future analysis employing the multi-seasonal ACTIVATE campaign will provide a valuable data set for investigations of this nature.

Data Availability Statement

Data sources are: CHECSM (<https://doi.org/10.6084/m9.figshare.11861859.v2>), CAMP²Ex (https://doi.org/10.5067/Airborne/CAMP2Ex_Aerosol_AircraftInSitu_P3_Data_1), ACTIVATE (http://doi.org/10.5067/ASDC/ACTIVATE_Aerosol_AircraftInSitu_Falcon_Data_1), AToM (<https://doi.org/10.3334/ORN-LDAAC/1748>), ICARTT and GoMACCS (<https://doi.org/10.6084/m9.figshare.14998278>), and other campaigns (https://figshare.com/articles/dataset/A_Multi-Year_Data_Set_on_Aerosol-Cloud-Precipitation-Meteorology_Interactions_for_Marine_Stratocumulus_Clouds/5099983).

References

- Andreae, M. O., & Crutzen, P. J. (1997). Atmospheric aerosols: Biogeochemical sources and role in atmospheric chemistry. *Science*, 276(5315), 1052–1058. <https://doi.org/10.1126/science.276.5315.1052>
- Barth, M. C., Rasch, P. J., Kiehl, J. T., Benkovitz, C. M., & Schwartz, S. E. (2000). Sulfur chemistry in the national center for atmospheric research community climate model: Description, evaluation, features, and sensitivity to aqueous chemistry. *Journal of Geophysical Research*, 105(D1), 1387–1415. <https://doi.org/10.1029/1999JD900773>
- Blando, J. D., & Turpin, B. J. (2000). Secondary organic aerosol formation in cloud and fog droplets: A literature evaluation of plausibility. *Atmospheric Environment*, 34(10), 1623–1632. [https://doi.org/10.1016/S1352-2310\(99\)00392-1](https://doi.org/10.1016/S1352-2310(99)00392-1)
- Boone, E. J., Laskin, A., Laskin, J., Wirth, C., Shepson, P. B., Stirm, B. H., & Pratt, K. A. (2015). Aqueous processing of atmospheric organic particles in cloud water collected via aircraft sampling. *Environmental Science and Technology*, 49(14), 8523–8530. <https://doi.org/10.1021/acs.est.5b01639>
- Canagaratna, M. R., Jayne, J. T., Jimenez, J. L., Allan, J. D., Alfarra, M. R., Zhang, Q., et al. (2007). Chemical and microphysical characterization of ambient aerosols with the aerodyne aerosol mass spectrometer. *Mass Spectrometry Reviews*, 26(2), 185–222. <https://doi.org/10.1002/mas.20115>

Acknowledgments

CAMP²Ex measurements and analysis were funded through NASA Grant 80NS-SC18K0148. ACTIVATE measurements and associated data analysis were funded by NASA Grant 80NSSC19K0442 in support of the ACTIVATE Earth Venture Suborbital-3 (EVS-3) investigation, which is funded by NASA's Earth Science Division and managed through the Earth System Science Pathfinder Program Office. ICARTT was funded by the National Science Foundation grant ATM-0340832. GoMACCS was funded by National Oceanic and Atmospheric Administration grant NA06OAR4310082. The other Twin Otter campaigns were funded by N00014-04-1-0118, N00014-10-1-0200, N00014-11-1-0783, N00014-10-1-0811, N00014-16-1-2567, and N00014-04-1-0018, with associated data analysis funded by N00014-21-1-2115. AToM SAGA measurements by Jack E. Dibb were funded by NASA grant NNX15AG62A.

- Carlton, A. G., Turpin, B. J., Altieri, K. E., Seitzinger, S. P., Mathur, R., Roselle, S. J., & Weber, R. J. (2008). CMAQ model performance enhanced when in-cloud secondary organic aerosol is included: Comparisons of organic carbon predictions with measurements. *Environmental Science and Technology*, 42(23), 8798–8802. <https://doi.org/10.1021/es801192n>
- Cautenet, S., & Lefeuvre, B. (1994). Contrasting behavior of gas and aerosol scavenging in convective rain: A numerical and experimental study in the African equatorial forest. *Journal of Geophysical Research*, 99(D6), 13013–13024. <https://doi.org/10.1029/93JD02712>
- Chebbi, A., & Carlier, P. (1996). Carboxylic acids in the troposphere, occurrence, sources, and sinks: A review. *Atmospheric Environment*, 30(24), 4233–4249. [https://doi.org/10.1016/1352-2310\(96\)00102-1](https://doi.org/10.1016/1352-2310(96)00102-1)
- Chesselet, R., Morelli, J., & Buat-Menard, P. (1972). Variations in ionic ratios between reference sea water and marine aerosols. *Journal of Geophysical Research*, 77(27), 5116–5131. <https://doi.org/10.1029/JC077i027p05116>
- Christian, T. J., Kleiss, B., Yokelson, R., Holzinger, R., & Crutzen, P. J. (2003). Comprehensive laboratory measurements of biomass-burning emissions: I. Emissions from Indonesian, African, and other fuels. *Journal of Geophysical Research*, 108(D23), 4719. <https://doi.org/10.1029/2003JD003704>
- Crahan, K. K., Hegg, D., Covert, D. S., & Jonsson, H. (2004). An exploration of aqueous oxalic acid production in the coastal marine atmosphere. *Atmospheric Environment*, 38(23), 3757–3764. <https://doi.org/10.1016/j.atmosenv.2004.04.009>
- Cruz, M. T., Bañaga, P. A., Betito, G., Braun, R. A., Stahl, C., Aghdam, M. A., et al. (2019). Size-resolved composition and morphology of particulate matter during the southwest monsoon in Metro Manila, Philippines. *Atmospheric Chemistry and Physics*, 19(16), 10675–10696. <https://doi.org/10.5194/acp-19-10675-2019>
- DeCarlo, P. F., Kimmel, J. R., Trimborn, A., Northway, M. J., Jayne, J. T., Aiken, A. C., et al. (2006). Field-deployable, high-resolution, time-of-flight aerosol mass spectrometer. *Analytical Chemistry*, 78(24), 8281–8289. <https://doi.org/10.1021/ac061249n>
- Dibb, J. E., Talbot, R. W., Scheuer, E. M., Seid, G., Avery, M. A., & Singh, H. B. (2003). Aerosol chemical composition in Asian continental outflow during the TRACE-P campaign: Comparison with PEM-West B. *Journal of Geophysical Research*, 108(D21). <https://doi.org/10.1029/2002JD003111>
- Dibb, J. E., Talbot, R. W., Seid, G., Jordan, C., Scheuer, E., Atlas, E., et al. (2002). Airborne sampling of aerosol particles: Comparison between surface sampling at Christmas Island and P-3 sampling during PEM-Tropics B. *Journal of Geophysical Research*, 107(D22–1), 2–17. <https://doi.org/10.1029/2001JD000408>
- Ervens, B. (2015). Modeling the processing of aerosol and trace gases in clouds and fogs. *Chemicals Reviews*, 42.
- Ervens, B., Sorooshian, A., Lim, Y. B., & Turpin, B. J. (2014). Key parameters controlling OH-initiated formation of secondary organic aerosol in the aqueous phase (aqSOA). *Journal of Geophysical Research: Atmospheres*, 119(7), 3997–4016. <https://doi.org/10.1002/2013JD021021>
- Ervens, B., Turpin, B. J., & Weber, R. J. (2011). Secondary organic aerosol formation in cloud droplets and aqueous particles (aqSOA): A review of laboratory, field and model studies. *Atmospheric Chemistry and Physics*, 11(21), 11069–11102. <https://doi.org/10.5194/acp-11-11069-2011>
- Faloon, I. (2009). Sulfur processing in the marine atmospheric boundary layer: A review and critical assessment of modeling uncertainties. *Atmospheric Environment*, 43(18), 2841–2854. <https://doi.org/10.1016/j.atmosenv.2009.02.043>
- Fehsenfeld, F. C., Ancellet, G., Bates, T. S., Goldstein, A. H., Hardesty, R. M., Honrath, R., et al. (2006). International consortium for atmospheric research on transport and transformation (ICARTT): North America to Europe-overview of the 2004 summer field study. *Journal of Geophysical Research*, 111(D23). <https://doi.org/10.1029/2006JD007829>
- Fu, T.-M., Jacob, D. J., Wittrock, F., Burrows, J. P., Vrekoussis, M., & Henze, D. K. (2008). Global budgets of atmospheric glyoxal and methylglyoxal, and implications for formation of secondary organic aerosols. *Journal of Geophysical Research*, 113(D15). <https://doi.org/10.1029/2007JD009505>
- Gonzalez, M. E., Stahl, C., Cruz, M. T., Bañaga, P. A., Betito, G., Braun, R. A., et al. (2021). Contrasting the size-resolved nature of particulate arsenic, cadmium, and lead among diverse regions. *Atmospheric Pollution Research*, 12(3), 352–361. <https://doi.org/10.1016/j.apr.2021.01.002>
- Hallquist, M., Wenger, J. C., Baltensperger, U., Rudich, Y., Simpson, D., Claeys, M., et al. (2009). The formation, properties and impact of secondary organic aerosol: Current and emerging issues. *Atmospheric Chemistry and Physics*, 9(14), 5155–5236. <https://doi.org/10.5194/acp-9-5155-2009>
- Heald, C. L., Coe, H., Jimenez, J. L., Weber, R. J., Bahreini, R., Middlebrook, A. M., et al. (2011). Exploring the vertical profile of atmospheric organic aerosol: Comparing 17 aircraft field campaigns with a global model. *Atmospheric Chemistry and Physics*, 11(24), 12673–12696. <https://doi.org/10.5194/acp-11-12673-2011>
- Heald, C. L., Jacob, D. J., Park, R. J., Russell, L. M., Huebert, B. J., Seinfeld, J. H., et al. (2005). A large organic aerosol source in the free troposphere missing from current models. *Geophysical Research Letters*, 32(18). <https://doi.org/10.1029/2005GL023831>
- Hennigan, C. J., Sullivan, A. P., Collett, J. L., & Robinson, A. L. (2010). Levoglucosan stability in biomass burning particles exposed to hydroxyl radicals. *Geophysical Research Letters*, 37(9). <https://doi.org/10.1029/2010GL043088>
- Hilario, M. R. A., Crosbie, E., Shook, M., Reid, J. S., Cambaliza, M. O. L., Simpas, J. B. B., et al. (2021). Measurement report: Long-range transport patterns into the tropical northwest Pacific during the CAMP²Ex aircraft campaign: Chemical composition, size distributions, and the impact of convection. *Atmospheric Chemistry and Physics*, 21(5), 3777–3802. <https://doi.org/10.5194/acp-21-3777-2021>
- Hilario, M. R. A., Cruz, M. T., Bañaga, P. A., Betito, G., Braun, R. A., Stahl, C., et al. (2020). Characterizing weekly cycles of particulate matter in a coastal megacity: The importance of a seasonal, size-resolved, and chemically-specified analysis. *Journal of Geophysical Research: Atmospheres*. <https://doi.org/10.1029/2020JD032614>
- Hilario, M. R. A., Cruz, M. T., Cambaliza, M. O. L., Reid, J. S., Xian, P., Simpas, J. B., et al. (2020). Investigating size-segregated sources of elemental composition of particulate matter in the South China Sea during the 2011 Vasco cruise. *Atmospheric Chemistry and Physics*, 20(3), 1255–1276. <https://doi.org/10.5194/acp-20-1255-2020>
- Hodzic, A., Kasibhatla, P. S., Jo, D. S., Cappa, C. D., Jimenez, J. L., Madronich, S., & Park, R. J. (2016). Rethinking the global secondary organic aerosol (SOA) budget: Stronger production, faster removal, shorter lifetime. *Atmospheric Chemistry and Physics*, 16(12), 7917–7941. <https://doi.org/10.5194/acp-16-7917-2016>
- Huang, D. D., Kong, L., Gao, J., Lou, S., Qiao, L., Zhou, M., et al. (2020). Insights into the formation and properties of secondary organic aerosol at a background site in Yangtze River Delta region of China: Aqueous-phase processing vs. photochemical oxidation. *Atmospheric Environment*, 239, 117716. <https://doi.org/10.1016/j.atmosenv.2020.117716>
- Huang, X.-F., & Yu, J. Z. (2007). Is vehicle exhaust a significant primary source of oxalic acid in ambient aerosols? *Geophysical Research Letters*, 34(2). <https://doi.org/10.1029/2006GL028457>
- Intergovernmental Panel on Climate Change. (2014). *Climate change 2014 mitigation of climate change: Working group III contribution to the fifth assessment report of the intergovernmental panel on climate change*. Cambridge University Press. <https://doi.org/10.1017/CBO9781107415416>
- Kanakidou, M., Seinfeld, J. H., Pandis, S. N., Barnes, I., Dentener, F. J., Facchini, M. C., et al. (2005). Organic aerosol and global climate modelling: A review. *Atmospheric Chemistry and Physics*, 5(4), 1053–1123. <https://doi.org/10.5194/acp-5-1053-2005>

- Kchih, H., Perrino, C., & Cherif, S. (2015). Investigation of desert dust contribution to source apportionment of PM₁₀ and PM_{2.5} from a southern mediterranean coast. *Aerosol and Air Quality Research*, *15*(2), 454–464. <https://doi.org/10.4209/aaqr.2014.10.0255>
- Kim, B.-G., Schwartz, S. E., Miller, M. A., & Min, Q. (2003). Effective radius of cloud droplets by ground-based remote sensing: Relationship to aerosol. *Journal of Geophysical Research*, *108*(D23). <https://doi.org/10.1029/2003JD003721>
- Kondo, Y., Matsui, H., Moteki, N., Sahu, L., Takegawa, N., Kajino, M., et al. (2011). Emissions of black carbon, organic, and inorganic aerosols from biomass burning in North America and Asia in 2008. *Journal of Geophysical Research*, *116*(D8), D08204. <https://doi.org/10.1029/2010JD015152>
- Liu, P. S. K., Leitch, W. R., Banic, C. M., Li, S.-M., Ngo, D., & Megaw, W. J. (1996). Aerosol observations at Chebogue Point during the 1993 North Atlantic regional experiment: Relationships among cloud condensation nuclei, size distribution, and chemistry. *Journal of Geophysical Research*, *101*(D22), 28971–28990. <https://doi.org/10.1029/96JD00445>
- Lu, M.-L., Conant, W. C., Jonsson, H. H., Varutbangkul, V., Flagan, R. C., & Seinfeld, J. H. (2007). The marine stratus/stratocumulus experiment (MASE): Aerosol-cloud relationships in marine stratocumulus. *Journal of Geophysical Research*, *112*(D10). <https://doi.org/10.1029/2006JD007985>
- Lu, M.-L., Sorooshian, A., Jonsson, H. H., Feingold, G., Flagan, R. C., & Seinfeld, J. H. (2009). Marine stratocumulus aerosol-cloud relationships in the MASE-II experiment: Precipitation susceptibility in eastern Pacific marine stratocumulus. *Journal of Geophysical Research*, *114*(D24), D24203. <https://doi.org/10.1029/2009JD012774>
- Mader, B. T., Yu, J. Z., Xu, J. H., Li, Q. F., Wu, W. S., Flagan, R. C., & Seinfeld, J. H. (2004). Molecular composition of the water-soluble fraction of atmospheric carbonaceous aerosols collected during ACE-Asia. *Journal of Geophysical Research*, *109*(D6). <https://doi.org/10.1029/2003JD004105>
- Marelle, L., Raut, J.-C., Thomas, J. L., Law, K. S., Quennehen, B., Ancellet, G., et al. (2015). Transport of anthropogenic and biomass burning aerosols from Europe to the Arctic during spring 2008. *Atmospheric Chemistry and Physics*, *15*(7), 3831–3850. <https://doi.org/10.5194/acp-15-3831-2015>
- Matsumoto, K., Uyama, Y., Hayano, T., Tanimoto, H., Uno, I., & Uematsu, M. (2003). Chemical properties and outflow patterns of anthropogenic and dust particles on Rishiri Island during the Asian Pacific regional aerosol characterization experiment (ACE-Asia). *Journal of Geophysical Research*, *108*(D23). <https://doi.org/10.1029/2003JD003426>
- May, A. A., McMeeking, G. R., Lee, T., Taylor, J. W., Craven, J. S., Burling, I., et al. (2014). Aerosol emissions from prescribed fires in the United States: A synthesis of laboratory and aircraft measurements. *Journal of Geophysical Research: Atmospheres*, *119*(20), 11826–11849. <https://doi.org/10.1002/2014JD021848>
- McNaughton, C. S., Clarke, A. D., Howell, S. G., Pinkerton, M., Anderson, B., Thornhill, L., et al. (2007). Results from the DC-8 inlet characterization experiment (DICE): Airborne versus surface sampling of mineral dust and sea salt aerosols. *Aerosol Science and Technology*, *41*(2), 136–159. <https://doi.org/10.1080/02786820601118406>
- McNeill, V. F. (2015). Aqueous organic chemistry in the atmosphere: Sources and chemical processing of organic aerosols. *Environmental Science and Technology*, *49*(3), 1237–1244. <https://doi.org/10.1021/es5043707>
- McVay, R., & Ervens, B. (2017). A microphysical parameterization of aqSOA and sulfate formation in clouds. *Geophysical Research Letters*, *44*(14), 7500–7509. <https://doi.org/10.1002/2017GL074233>
- Mochida, M., Kawabata, A., Kawamura, K., Hatsushika, H., & Yamazaki, K. (2003). Seasonal variation and origins of dicarboxylic acids in the marine atmosphere over the western North Pacific. *Journal of Geophysical Research*, *108*(D6), 4193. <https://doi.org/10.1029/2002JD002355>
- Murphy, D. M., Cziczo, D. J., Froyd, K. D., Hudson, P. K., Matthew, B. M., Middlebrook, A. M., et al. (2006). Single-particle mass spectrometry of tropospheric aerosol particles. *Journal of Geophysical Research*, *111*(D23). <https://doi.org/10.1029/2006JD007340>
- Murphy, D. M., Froyd, K. D., Bian, H., Brock, C. A., Dibb, J. E., DiGangi, J. P., et al. (2019). The distribution of sea-salt aerosol in the global troposphere. *Atmospheric Chemistry and Physics*, *19*(6), 4093–4104. <https://doi.org/10.5194/acp-19-4093-2019>
- Myriokefalitakis, S., Tsigaridis, K., Mihalopoulos, N., Sciare, J., Nenes, A., Kawamura, K., et al. (2011). In-cloud oxalate formation in the global troposphere: A 3-D modeling study. *Atmospheric Chemistry and Physics*, *11*(12), 5761–5782. <https://doi.org/10.5194/acp-11-5761-2011>
- Nah, T., Guo, H., Sullivan, A. P., Chen, Y., Tanner, D. J., Nenes, A., et al. (2018). Characterization of aerosol composition, aerosol acidity, and organic acid partitioning at an agriculturally intensive rural southeastern US site. *Atmospheric Chemistry and Physics*, *18*(15), 11471–11491. <https://doi.org/10.5194/acp-18-11471-2018>
- Narukawa, M., Kawamura, K., Takeuchi, N., & Nakajima, T. (1999). Distribution of dicarboxylic acids and carbon isotopic compositions in aerosols from 1997 Indonesian forest fires. *Geophysical Research Letters*, *26*(20), 3101–3104. <https://doi.org/10.1029/1999GL010810>
- Pai, S. J., Heald, C. L., Pierce, J. R., Farina, S. C., Marais, E. A., Jimenez, J. L., et al. (2020). An evaluation of global organic aerosol schemes using airborne observations. *Atmospheric Chemistry and Physics*, *20*(5), 2637–2665. <https://doi.org/10.5194/acp-20-2637-2020>
- Pang, H., Zhang, Q., Wang, H., Cai, D., Ma, Y., Li, L., et al. (2019). Photochemical aging of guaiacol by Fe(III)–Oxalate complexes in atmospheric aqueous phase. *Environmental Science and Technology*, *53*(1), 127–136. <https://doi.org/10.1021/acs.est.8b04507>
- Park, S. H., Song, C. B., Kim, M. C., Kwon, S. B., & Lee, K. W. (2004). Study on size distribution of total aerosol and water-soluble ions during an asian dust storm event at Jeju Island, Korea. *Environmental Monitoring and Assessment*, *93*(1), 157–183. <https://doi.org/10.1023/B:EMAS.0000016805.04194.56>
- Parrish, D. D., Allen, D. T., Bates, T. S., Estes, M., Fehsenfeld, F. C., Feingold, G., et al. (2009). Overview of the second Texas air quality study (TexAQS II) and the Gulf of Mexico atmospheric composition and climate study (GoMACCS). *Journal of Geophysical Research*, *114*, D00F13. <https://doi.org/10.1029/2009JD011842>
- Pósfai, M., Simonics, R., Li, J., Hobbs, P. V., & Buseck, P. R. (2003). Individual aerosol particles from biomass burning in southern Africa: 1. Compositions and size distributions of carbonaceous particles. *Journal of Geophysical Research*, *108*(D13), D138483. <https://doi.org/10.1029/2002JD002291>
- Putaud, J., Raes, F., Van Dingenen, R., Brüggemann, E., Facchini, M., Decesari, S., et al. (2004). European aerosol phenomenology—2: Chemical characteristics of particulate matter at kerbside, urban, rural and background sites in Europe. *Atmospheric Environment*, *38*(16), 2579–2595. <https://doi.org/10.1016/j.atmosenv.2004.01.041>
- Rinaldi, M., Decesari, S., Carbone, C., Finessi, E., Fuzzi, S., Ceburnis, D., et al. (2011). Evidence of a natural marine source of oxalic acid and a possible link to glyoxal. *Journal of Geophysical Research*, *116*(D16), D16204. <https://doi.org/10.1029/2011JD015659>
- Roberts, G. C., Andreae, M. O., Zhou, J., & Artaxo, P. (2001). Cloud condensation nuclei in the Amazon Basin: “Marine” conditions over a continent? *Geophysical Research Letters*, *28*(14), 2807–2810. <https://doi.org/10.1029/2000GL012585>
- Saxena, P., & Hildemann, L. M. (1996). Water-soluble organics in atmospheric particles: A critical review of the literature and application of thermodynamics to identify candidate compounds. *Journal of Atmospheric Chemistry*, *24*(1), 57–109. <https://doi.org/10.1007/BF00053823>

- Schlosser, J. S., Dadashazar, H., Edwards, E.-L., Mardi, A. H., Prabhakar, G., Stahl, C., et al. (2020). Relationships between supermicrometer sea salt aerosol and marine boundary layer conditions: Insights from repeated identical flight patterns. *Journal of Geophysical Research: Atmospheres*, *125*(12), e2019JD032346. <https://doi.org/10.1029/2019JD032346>
- Schroder, J. C., Campuzano-Jost, P., Day, D. A., Shah, V., Larson, K., Sommers, J. M., et al. (2018). Sources and secondary production of organic aerosols in the Northeastern United States during WINTER. *Journal of Geophysical Research: Atmospheres*. <https://doi.org/10.1029/2018JD028475>
- Sorooshian, A., Anderson, B., Bauer, S. E., Braun, R. A., Cairns, B., Crosbie, E., et al. (2019). Aerosol–cloud–meteorology interaction airborne field investigations: Using lessons learned from the U.S. West Coast in the Design of ACTIVATE off the U.S. East Coast. *Bulletin of the American Meteorological Society*, *100*(8), 1511–1528. <https://doi.org/10.1175/BAMS-D-18-0100.1>
- Sorooshian, A., Brechtel, F. J., Ma, Y., Weber, R. J., Corless, A., Flagan, R. C., & Seinfeld, J. H. (2006). Modeling and characterization of a particle-into-liquid sampler (PILS). *Aerosol Science and Technology*, *40*(6), 396–409. <https://doi.org/10.1080/02786820600632282>
- Sorooshian, A., Corral, A. F., Braun, R. A., Cairns, B., Crosbie, E., Ferrare, R., et al. (2020). Atmospheric research over the western North Atlantic Ocean region and North American East Coast: A review of past work and challenges ahead. *Journal of Geophysical Research: Atmospheres*, *125*(6), e2019JD031626. <https://doi.org/10.1029/2019JD031626>
- Sorooshian, A., Crosbie, E., Maudlin, L. C., Youn, J.-S., Wang, Z., Shingler, T., et al. (2015). Surface and airborne measurements of organosulfur and methanesulfonate over the western United States and coastal areas. *Journal of Geophysical Research: Atmospheres*, *120*(16), 8535–8548. <https://doi.org/10.1002/2015JD023822>
- Sorooshian, A., Lu, M.-L., Brechtel, F. J., Jonsson, H., Feingold, G., Flagan, R. C., & Seinfeld, J. H. (2007). On the source of organic acid aerosol layers above clouds. *Environmental Science and Technology*, *41*(13), 4647–4654. <https://doi.org/10.1021/es0630442>
- Sorooshian, A., Murphy, S. M., Hersey, S., Bahreini, R., Jonsson, H., Flagan, R. C., & Seinfeld, J. H. (2010). Constraining the contribution of organic acids and AMS m/z 44 to the organic aerosol budget: On the importance of meteorology, aerosol hygroscopicity, and region. *Geophysical Research Letters*, *37*(21). <https://doi.org/10.1029/2010GL044951>
- Sorooshian, A., Ng, N. L., Chan, A. W. H., Feingold, G., Flagan, R. C., & Seinfeld, J. H. (2007). Particulate organic acids and overall water-soluble aerosol composition measurements from the 2006 Gulf of Mexico atmospheric composition and climate study (GoMACCS). *Journal of Geophysical Research*, *112*(D13). <https://doi.org/10.1029/2007JD008537>
- Sorooshian, A., Padró, L. T., Nenes, A., Feingold, G., McComiskey, A., Hersey, S. P., et al. (2009). On the link between ocean biota emissions, aerosol, and maritime clouds: Airborne, ground, and satellite measurements off the coast of California. *Global Biogeochemical Cycles*, *23*(4), GB4007. <https://doi.org/10.1029/2009GB003464>
- Sorooshian, A., Varutbangkul, V., Brechtel, F. J., Ervens, B., Feingold, G., Bahreini, R., et al. (2006). Oxalic acid in clear and cloudy atmospheres: Analysis of data from international consortium for atmospheric research on transport and transformation 2004. *Journal of Geophysical Research*, *111*(D23), D23S45. <https://doi.org/10.1029/2005JD006880>
- Sorooshian, A., Wang, Z., Coggon, M. M., Jonsson, H. H., & Ervens, B. (2013). Observations of sharp oxalate reductions in stratocumulus clouds at variable altitudes: Organic acid and metal measurements during the 2011 E-PEACE campaign. *Environmental Science and Technology*, *47*(14), 7747–7756. <https://doi.org/10.1021/es4012383>
- Stahl, C., Crosbie, E., Bañaga, P. A., Betito, G., Braun, R. A., Cainglet, Z. M., et al. (2021). Total organic carbon and the contribution from spatiotemporal organics in cloud water: Airborne data analysis from the CAMP²Ex field campaign. *Atmospheric Chemistry and Physics*, *21*(18), 14109–14129. <https://doi.org/10.5194/acp-21-14109-2021>
- Stahl, C., Cruz, M. T., Bañaga, P. A., Betito, G., Braun, R. A., Aghdam, M. A., et al. (2020a). An annual time series of weekly size-resolved aerosol properties in the megacity of Metro Manila, Philippines. *Scientific Data*, *7*(1), 128. <https://doi.org/10.1038/s41597-020-0466-y>
- Stahl, C., Cruz, M. T., Bañaga, P. A., Betito, G., Braun, R. A., Aghdam, M. A., et al. (2020b). Sources and characteristics of size-resolved particulate organic acids and methanesulfonate in a coastal megacity: Manila, Philippines. *Atmospheric Chemistry and Physics*, *20*(24), 15907–15935. <https://doi.org/10.5194/acp-20-15907-2020>
- Sullivan, R. C., & Prather, K. A. (2007). Investigations of the diurnal cycle and mixing state of oxalic acid in individual particles in asian aerosol outflow. *Environmental Science and Technology*, *41*(23), 8062–8069. <https://doi.org/10.1021/es071134g>
- Švédová, B., Kucbel, M., Raclavská, H., Růžičková, J., Raclavský, K., & Sassmanová, V. (2019). Water-soluble ions in dust particles depending on meteorological conditions in urban environment. *Journal of Environmental Management*, *237*, 322–331. <https://doi.org/10.1016/j.jenvman.2019.02.086>
- Swan, H. B., & Ivey, J. P. (2021). Elevated particulate methanesulfonate, oxalate and iron over Sydney Harbour in the austral summer of 2019–20 during unprecedented bushfire activity. *Atmospheric Environment*, *266*, 118739. <https://doi.org/10.1016/j.atmosenv.2021.118739>
- Tao, Y., & Murphy, J. G. (2019). The mechanisms responsible for the interactions among oxalate, pH, and Fe dissolution in PM_{2.5}. *ACS Earth and Space Chemistry*, *3*(10), 2259–2265. <https://doi.org/10.1021/acsearthspacechem.9b00172>
- Turekian, V. C., Macko, S. A., & Keene, W. C. (2003). Concentrations, isotopic compositions, and sources of size-resolved, particulate organic carbon and oxalate in near-surface marine air at Bermuda during spring. *Journal of Geophysical Research*, *108*(D5). <https://doi.org/10.1029/2002JD002053>
- Wang, G., Kawamura, K., Cheng, C., Li, J., Cao, J., Zhang, R., et al. (2012). Molecular distribution and stable carbon isotopic composition of dicarboxylic acids, ketocarboxylic acids, and α -dicarbonyls in size-resolved atmospheric particles from Xi'an city, China. *Environmental Science and Technology*, *46*(9), 4783–4791. <https://doi.org/10.1021/es204322c>
- Wang, Q., Dong, X., Fu, J. S., Xu, J., Deng, C., Jiang, Y., et al. (2018). Environmentally dependent dust chemistry of a super Asian dust storm in March 2010: Observation and simulation. *Atmospheric Chemistry and Physics*, *18*(5), 3505–3521. <https://doi.org/10.5194/acp-18-3505-2018>
- Warneck, P. (2003). In-cloud chemistry opens pathway to the formation of oxalic acid in the marine atmosphere. *Atmospheric Environment*, *37*(17), 2423–2427. [https://doi.org/10.1016/S1352-2310\(03\)00136-5](https://doi.org/10.1016/S1352-2310(03)00136-5)
- Weber, R. J., Orsini, D., Daun, Y., Lee, Y.-N., Klotz, P. J., & Brechtel, F. (2001). A particle-into-liquid collector for rapid measurement of aerosol bulk chemical composition. *Aerosol Science and Technology*, *35*(3), 718–727. <https://doi.org/10.1080/02786820152546761>
- Wofsy, S. C., Afshar, S., Allen, H. M., Apel, E. C., Asher, E. C., Barletta, B., et al. (2018). *ATOM: Merged Atmospheric Chemistry, Trace Gases, and Aerosols [Dataset]*. ORNL DAAC. <https://doi.org/10.3334/ORNLDAAC/1581>
- Wonaschuetz, A., Sorooshian, A., Ervens, B., Chuang, P. Y., Feingold, G., Murphy, S. M., et al. (2012). Aerosol and gas re-distribution by shallow cumulus clouds: An investigation using airborne measurements. *Journal of Geophysical Research*, *117*(D17), D17202. <https://doi.org/10.1029/2012JD018089>
- Yang, F., Gu, Z., Feng, J., Liu, X., & Yao, X. (2014). Biogenic and anthropogenic sources of oxalate in PM_{2.5} in a mega city, Shanghai. *Atmospheric Research*, *138*, 356–363. <https://doi.org/10.1016/j.atmosres.2013.12.006>
- Yao, X., Fang, M., Chan, C. K., Ho, K. F., & Lee, S. C. (2004). Characterization of dicarboxylic acids in PM_{2.5} in Hong Kong. *Atmospheric Environment*, *38*(7), 963–970. <https://doi.org/10.1016/j.atmosenv.2003.10.048>

- Yao, X., Lau, A. P. S., Fang, M., Chan, C. K., & Hu, M. (2003). Size distributions and formation of ionic species in atmospheric particulate pollutants in Beijing, China: 2—Dicarboxylic acids. *Atmospheric Environment*, *37*(21), 3001–3007. [https://doi.org/10.1016/S1352-2310\(03\)00256-5](https://doi.org/10.1016/S1352-2310(03)00256-5)
- Yu, J. Z., Huang, X.-F., Xu, J., & Hu, M. (2005). When aerosol sulfate goes up, so does oxalate: Implication for the formation mechanisms of oxalate. *Environmental Science and Technology*, *39*(1), 128–133. <https://doi.org/10.1021/es049559f>
- Zhang, Q., Alfarra, M. R., Worsnop, D. R., Allan, J. D., Coe, H., Canagaratna, M. R., & Jimenez, J. L. (2005). Deconvolution and quantification of hydrocarbon-like and oxygenated organic aerosols based on aerosol mass spectrometry. *Environmental Science and Technology*, *39*(13), 4938–4952. <https://doi.org/10.1021/es048568l>
- Zhang, Q., Jimenez, J. L., Canagaratna, M. R., Allan, J. D., Coe, H., Ulbrich, I., et al. (2007). Ubiquity and dominance of oxygenated species in organic aerosols in anthropogenically-influenced Northern Hemisphere midlatitudes. *Geophysical Research Letters*, *34*(13). <https://doi.org/10.1029/2007GL029979>
- Zhang, C., Yang, C., Liu, X., Cao, F., & Zhang, Y. (2020). Insight into the photochemistry of atmospheric oxalate through hourly measurements in the northern suburbs of Nanjing, China. *The Science of the Total Environment*, *719*, 137416. <https://doi.org/10.1016/j.scitotenv.2020.137416>
- Zhan, B., Zhong, H., Chen, H., Chen, Y., Li, X., Wang, L., et al. (2021). The roles of aqueous-phase chemistry and photochemical oxidation in oxygenated organic aerosols formation. *Atmospheric Environment*, *266*, 118738. <https://doi.org/10.1016/j.atmosenv.2021.118738>
- Zhou, Y., Huang, X. H., Bian, Q., Griffith, S. M., Louie, P. K. K., & Yu, J. Z. (2015). Sources and atmospheric processes impacting oxalate at a suburban coastal site in Hong Kong: Insights inferred from 1 year hourly measurements. *Journal of Geophysical Research: Atmospheres*, *120*(18), 9772–9788. <https://doi.org/10.1002/2015JD023531>
- Zhou, Y., Zhang, Y., Griffith, S. M., Wu, G., Li, L., Zhao, Y., et al. (2020). Field evidence of Fe-mediated photochemical degradation of Oxalate and subsequent sulfate formation observed by single particle mass spectrometry. *Environmental Science and Technology*, *54*(11), 6562–6574. <https://doi.org/10.1021/acs.est.0c00443>
- Zhu, J., & Penner, J. E. (2019). Global modeling of secondary organic aerosol with organic nucleation. *Journal of Geophysical Research: Atmospheres*, *124*(14), 8260–8286. <https://doi.org/10.1029/2019JD030414>
- Ziemba, L. D., Griffin, R. J., Whitlow, S., & Talbot, R. W. (2011). Characterization of water-soluble organic aerosol in coastal New England: Implications of variations in size distribution. *Atmospheric Environment*, *45*(39), 7319–7329. <https://doi.org/10.1016/j.atmosenv.2011.08.022>